

---

## A Second Level Trigger for PAMELA

---

J. Lundquist,<sup>1</sup> M. Boezio,<sup>2</sup> V. Bonvicini,<sup>2</sup> P. Carlson,<sup>1</sup> J. Lund,<sup>1</sup> A. Menicucci,<sup>3</sup> S. Orsi,<sup>1</sup> M. Pearce,<sup>1</sup> P. Picozza,<sup>3</sup> P. Schiavon,<sup>2</sup> A. Vacchi,<sup>2</sup> G. Zampa,<sup>2</sup> N. Zampa,<sup>2</sup>  
(1) *Department of Physics, The Royal Institute of Technology (KTH), AlbaNova Universitetscentrum, Stockholm, Sweden*  
(2) *INFN section and Physics Department, University of Trieste, Trieste, Italy*  
(3) *INFN section and Physics Department, University of Tor Vergata, Roma, Italy*

---

### Abstract

The PAMELA telescope will be installed on-board the Resurs-DK satellite and launched at the beginning of 2004. The satellite will fly for at least 3 years in a quasi-polar orbit. A second level trigger has been designed to reduce the amount of data and dead time due to false triggers produced by particles outside the PAMELA acceptance interacting with the payload structure. These events will be rejected using the information from the anticoincidence system (AC) that surrounds the PAMELA spectrometer. The AC information will be combined with that from the calorimeter allowing events showering in the calorimeter and produces a signal in the AC due to backscattered particles to be retained. The design of the second level trigger and its performance from simulations and test beam data is presented.

### 1. The PAMELA Experiment

PAMELA [4] is a satellite-borne experiment primarily designed to measure the properties of antimatter in the cosmic radiation. PAMELA comprises of a transition radiation detector, a permanent magnet/silicon tracker, a Si-W imaging calorimeter, a time-of-flight (ToF) system and anticoincidence veto shield. PAMELA will be carried by the Resurs-DK1 polar orbiting satellite. The planned launch date is in early 2004.

The AC system [5] is composed of a top detector, CAT, and four side detectors, CAS. In this study only the CAS detectors have been used. Each detector is made from a sheet of 8mm thick plastic scintillator read out by photomultiplier tubes. The CAS detectors surround the spectrometer (tracker and magnet) and help to reject out-of-acceptance triggers.

The sampling calorimeter [2] is made from silicon sensor planes interleaved with tungsten absorbers. The traverse resolution is given by the segmentation of

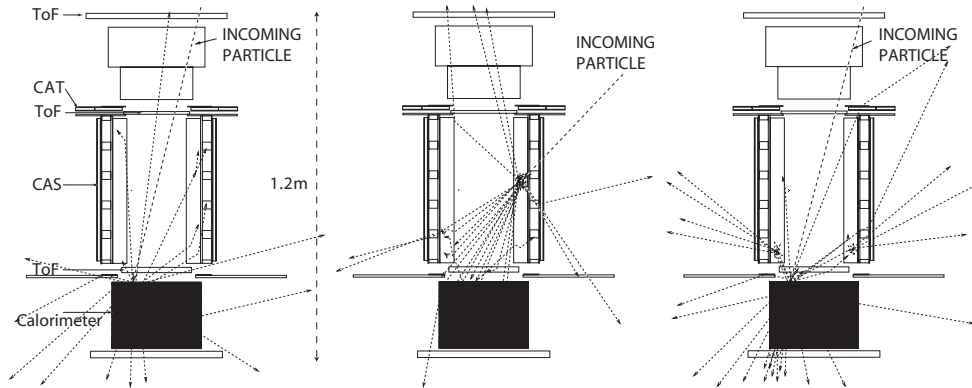


**Fig. 1.** Event types: (left, a) a 'good' trigger, (middle, b) a 'false' trigger, (right, c) a backscattering event

the silicon detectors. The segmentation is made in 32 strips with a width of 2.4 mm. Each tungsten plane is sandwiched between two layers of silicon detectors. Either view (X or Y) is composed of a square matrix of  $3 \times 3$  detectors and each strip is connected to the those belonging to the two detectors of the same row (or column). The data from the calorimeter front end boards are processed by four DSPs (Digital Signal Processors). One DSP takes care of data from either an even or odd numbered X or Y plane. In both the X and Y direction there are 22 planes. Each DSP is receiving signals from 11 planes (here called a sector). In figure 1 relative positions of the CAS detectors and the calorimeter are shown.

## 2. Trigger Types

In this study the condition for a first level trigger is that a signal  $>0.25$  mip is deposited coincidentally in each ToF scintillator. A first level trigger can include both 'good' triggers, i.e. particles entering and traversing the tracker acceptance and reaching the calorimeter without interacting, and 'false' triggers, i.e. particles hitting the experiment from outside the acceptance or interacting with the inside of the tracker cavity. In figure 1 a and b these two types of triggers are illustrated. To examine the performance of the AC system, a simulation study has been performed. The simulations included protons of various energies generated at locations situated above, on the side of, and below the experiment. The dominant component of the 'false' triggers are produced by particles hitting the experiment from above, but a non-negligible component comes from particles hitting the experiment from the sides and from below. By using the AC system in a second level trigger one can reduce this background significantly with the condition that a level one trigger should not be accompanied by a signal in any of the AC detectors.

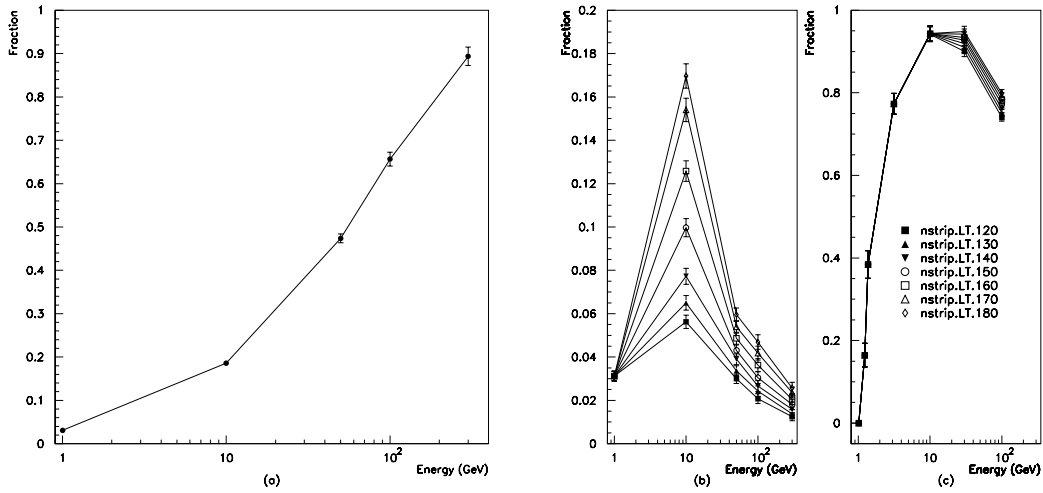


**Fig. 2.** a) Backscattering ratio with only AC rejection (electrons), b) Backscattering ratio with combined AC and calorimeter rejection (electrons), c) Rejection ratio with combined AC and calorimeter rejection (protons)

### 3. Backscattering

An event where a particle passes cleanly through the spectrometer can still give rise to an AC signal due to backscattered particles produced in the calorimeter (see figure 1c). Using the AC system to reject 'false' triggers in this simple way will therefore result in loss of 'good' events. To estimate the effect of backscattering, electrons were simulated entering the apparatus from above in the PAMELA acceptance. As shown in figure 2a the fraction of rejected 'good' triggers increases significantly with the energy of the incident particles as expected. Considering that high energy electrons are much less abundant than low energy ones it's necessary to avoid using selections that have high inefficiencies.

In this study the energy deposition in the the calorimeter was used to provide a variable sensitive to the development of the shower. The calorimeter variable used was the total number of strips that were hit for each sector (11 planes). A revised second level trigger condition was then formed, i.e.: signal in AC and no activity in any of the 4 calorimeter sectors above a predefined cut-off. A range of cut-offs were investigated from 120-180 (out of 1056) strips. In figure 2b the fraction of rejected 'good' triggers is plotted for the 8 different cuts-offs in the strip variable. As seen in this figure the fraction of lost 'good' events is greatly reduced (especially at higher energies). The effect of the these cuts on the rejection of 'false' proton triggers is shown in figure 2c.

When combined with the proton spectrum for the polar region of the orbit

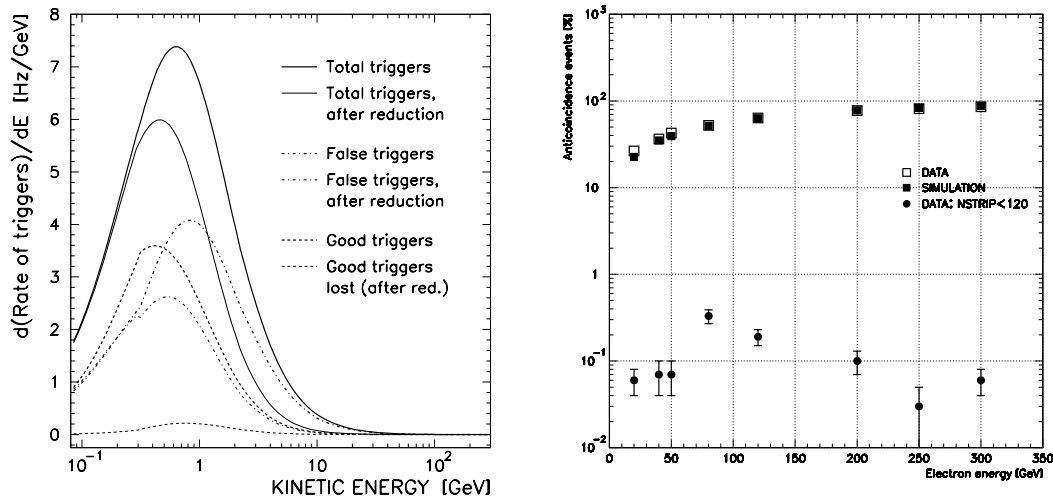


**Fig. 3.** (left) trigger rates, (right) results from the testbeam study

[1], where the proton flux has its maximum, the resulting trigger rate becomes as shown in figure 3 (left). The total integrated trigger rate after reduction is 11.6 Hz for a cut-off of 120 strips. It can also be seen that the 'false' trigger rate can be reduced significantly (integration gives a total reduction by 70%) without losing any significant part of the 'good' events.

In July 2002 a test beam study was performed at CERN in the H4 beam line. An electron beam of various energies was aimed at the center of the PAMELA acceptance. In figure 3 (right) the full circles show the measured ratio where an AC rejection combined with a calorimeter cut-off of 120 strips has been imposed. The full squares shows the same but without the calorimeter condition. They can be compared with the backscattering estimated from a simulation of the test beam AC (open squares) and a good agreement can be noticed. Additional comparison between experimental and simulated AC performance can be found in [3].

#### 4. References

1. Alcaraz J. et al., 2000, Phys. Lett. B 472, 215
2. Boezio M. et al., 2002, Nucl. Inst. and Meth. A 487, 407
3. Lund J. et al., these proceedings
4. Pearce M., 2002, Nucl. Phys. B 113, 314
5. Pearce M. et al., these proceedings